THE GENESIS OF THE RADIAL TIDAL CURRENT OFF THE CENTRAL JIANGSU COAST

P. Yao[1,3], Z.B. Wang[1,2], C.K. Zhang[3], M. Su[1,3], Y.P. Chen[3], M.J.F. Stive[1]

Abstract

One of the characteristics of the radial sand ridge field (RSRF) in the South Yellow Sea off the Jiangsu coast is the distinctive radial tidal current field. Although many studies have focused on the hydrodynamic environment around radial sand ridges, the knowledge on the genesis of the radial tidal current is still in a very basic stage. This paper attempts to explore the formation mechanism of the local radial tidal current field by a schematized process-based model. Two factors which are hypothesized to be responsible for the radial tidal current pattern are investigated: coastline shape, and the submarine topography. The results show that the schematized model sufficiently represents the real pattern of the tidal wave propagation in the South Yellow Sea. A preliminary description of the formation mechanism and main influence factors are obtained through sensitive analysis.

Key words: radial tidal current field, radial sand ridges, formation mechanism, schematized model, tidal wave

1. Introduction

In the central Jiangsu coast, there are a series of radiating sand bodies taken the city of Jianggang as a center. These sand bodies are known as radial sand ridge field (subsequently referred to as RSRF) which cover an area of 22470 km^2 and are made up of 70 different sizes of sand ridges (Wang, 2003). These ridges are considered to be very useful potential land resources in the future. So, it is very important to improve the understanding on its formation, maintenance and evolution in both academic and practical interest (Ren et al., 1986).

The processes around the RSRF area are very complicated, covering the interaction between various hydraulic forcing, sediment transport and biological dynamics. Tidal currents are considered to play an important role in the formation and the maintenance of the RSRF, while the effect of waves and other hydrodynamic forces are relatively one order of magnitude less (Liu and Xia, 2004; Wang, 2003). So, most studies have focused on the tidal dynamics and the corresponding morphological change based on both field observation and numerical modeling (Ren et al., 1986; Zhang and Zhang, 1996; Zhu, 1998; Zhu et al. 1998). Zhang et al. (1999) proposed a very classic theory on the dynamic mechanism of the RSRF area, which can be summarized as "Tidal current-induced formation--storm-induced change--tidal current-induced recovery".

According to field observations and numerical simulations, an important tidal current features in the RSRF area is: the tidal current will converge and diverge in the radial sand ridge field during flood and ebb tide respectively. As the pattern of the tidal current field is the same with the distribution of the radial sand ridges, this phenomenon raises an academic controversial on the relationship between the radial tidal current and the RSRF: the local special bathymetry influenced the tidal current field or the radial current field shaped the local radial topography.

Researchers who hold the former opinion thought that tidal current field were first caused by the radial seabed topography, and then the formation of radial current field influenced the local seabed topography and this feedback mechanism gradually formed the radial sand ridges. The essence of this view is that the shape of ridges are decided by the initial seabed topography which was formed by geological changes

[1] Faculty of Civil Engineering and Geosciences, Section of Hydraulic Engineering, Delft University of Technology, P.O.Box 5048, 2600 GA, Delft, The Netherlands. P.Yao@tudelft.nl, M.J.F.Stive@tudelft.nl, M.Su@tudelft.nl
[2] Deltares, P.O.Box 177, 2600 MH Delft, The Netherlands. Zheng.Wang@deltares.nl
[3] College of Harbour, Coastal and Offshore Engineering, Hohai University, 1 Xikang Road, Nanjing 210098, China. CKZhang@hhu.edu.cn, ypchen@hhu.edu.cn

during Holocene transgression, and the effect of the current field is to make the ridges distribution more perfect (Li and Li, 1981; Wan and Zhang, 1985; Zhang, 1991). Another view is that the special tidal current pattern is not only independent of the local bathymetry, but also playing an crucial role in the formation of radial sand ridge system (Wang, 2003; Yang, 1985; Zhang and Li, 1999; Zhu and Chang, 2001, 1997; Zhu and Yan, 1998; Zhu et al., 1995). Song et al. (1998) and Zhu and Chang (1997) successfully simulated the radial current pattern under the conditions of the flat seabed and a linear sloped topography using numerical modeling. Additionally, the simulation of Paleo-tidal current field in South Yellow Sea also proved that this special current pattern existed 7000 years ago and the pattern has been very stable since the Holocene transgression period (Zhu, 1998).

At present, the description of the tidal current pattern which is suggested by many researchers is: the radial tidal current field caused by the meet of the two tidal wave systems—rotating tidal wave system in the South Yellow Sea and the incident tidal wave from the east China. However, the knowledge of the radial flow pattern is limited to this view, and no deep understandings are found in literatures. The factors which may influence the formation and maintenance of the tidal current field is still not clear.

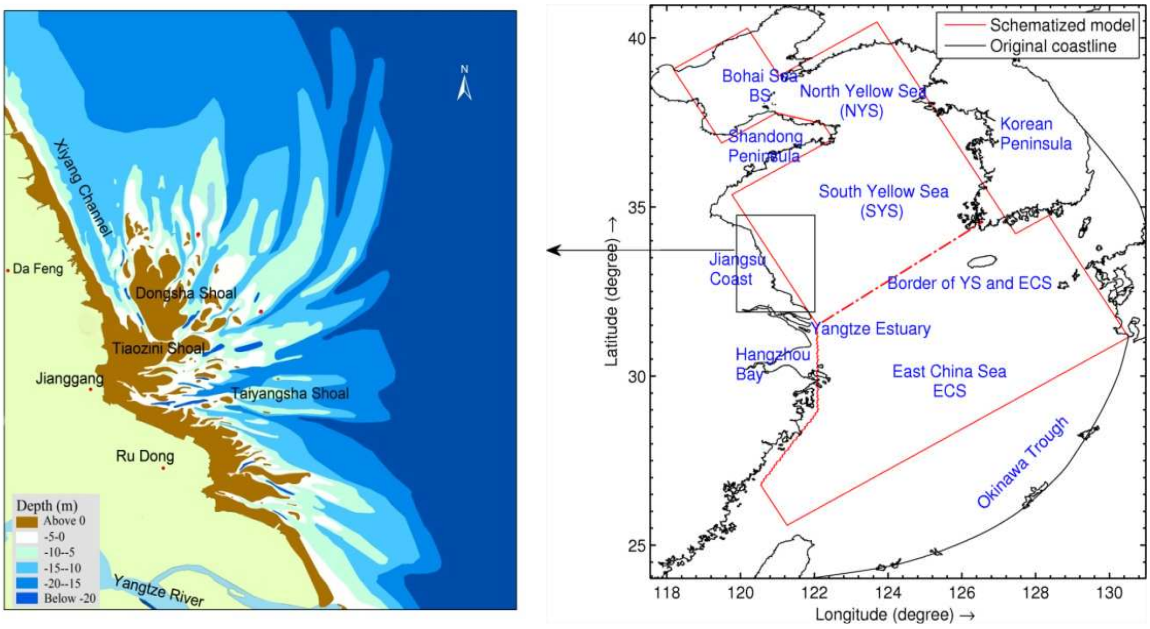

Figure 1. The study area and the model domain (right), and the radial sand ridge field (left). Note: BS = Bohai Sea; NYS = North Yellow Sea; SYS = South Yellow Sea; ECS = East China Sea

On the other hand, some idealized analytical models are proposed to obtain more deep insight on the tidal dynamics in such shallow water zones like the East China Sea, the North Sea etc. Compared with the numerical solutions, the analytical solutions on the idealized basin are very helpful to distinguish the influence factors on the tidal dynamics. The classic analytic solution for tidal waves in a rectangular basin of uniform depth was first obtained by Taylor (1922). Taylor considered that the tidal wave in a semi-enclosed basin consists of a linear superposition of incident and reflected Kelvin waves and an infinite number of Poincare waves. Kang (1984) first used a rectangular basin with an opening at the head to represent the South Yellow Sea and investigated the asymmetry of the amphidromic system. He found the asymmetry of amphidromic system arises primarily due to a partial penetration of tidal energy through the opening at the bay head. Ye and Chen (1987) examined the effect of the seabed topography on tidal amphidromic system. He found that in the shallow water zones, the shift of the amphidromic points is mainly due to bottom friction, while in waters having greater average depths, the effect of the topography is becoming the main factor. The study of Jung et al. (2005) also shows the variations in depth, bottom friction and the open heading in the boundary conditions all contribute to the determination of the formation of amphidromic points as well as overall patterns of M_2 tidal distribution. With the help of the analytic method, the tidal dynamics and the corresponding influence factors can be well investigated.

However, this method used many unavoidable hypotheses and is only applied in idealized condition.

Most numerical modeling are focusing on the tide dynamics and the local morphological changes, whereas the analytic solutions concentrate on the tidal wave dynamics under different influencing factors. However, very little are focusing on the formation mechanism of the radial tidal current. Therefore, we are planning to combine the method of the analytic solutions and the numerical modeling, in order to study the formation mechanism of the radial pattern of the tidal current through analyzing the different influence factors. In this study, we first develop a schematized process-based model to analyze the tidal dynamics with the consideration of the analytical method. Several experiments are carried out to test the sensitivity of the tidal currents under different conditions.

2. Model Setup

In the former analytical solutions of the tidal dynamic pattern in the South Yellow Sea, the domain is often simplified to be a regular tidal basin with uniform or linear water depth. In our numerical modeling, we take advantage of the method used in analytical models, and first simplify the domain of the Chinese marginal sea to be a regular basin, but using more actual bathymetry. The schematized 2D model is developed based on Delft3D modeling system Lesser et al. (2004). Delft3D fully integrates the effects of waves, tide and sediment with on line morphological update in coastal, river and estuarine regions. Here, we only consider the tide neglecting the waves and sediment, because the scale of the study area is relative large and our aim is focusing more on the tidal current pattern.

2.1. *Model domain and boundary conditions*

The schematized model domain covers the area of the whole Chinese marginal seas (Figure 1). The irregular coastlines are changed to be straight lines but following the trend of the coast and keeping the main features. Through this simplification, the general shape of most of the Chinese coastline is conserved, for example, the shape of Shandong Peninsula, Yangtze River Estuary and Hangzhou Bay etc. In addition, the Bohai Sea has been idealized as a rectangular basin, and this simplification has little influence on the tidal wave pattern in the South Yellow Sea, because the incoming tidal energy to the Bohai Sea from the Yellow Sea only account for 6.86% of that into the Yellow Sea from the East China Sea (Fang, 1979). As the model is schematized to investigate different factors such as the shape of the coastline, water depth etc., the shape of the model domain is not fixed in sensitivity experiments.

The model used the rectangular grid with a grid size of 3’×3’ approximately, under the spherical coordinate. The bathymetry of the model is generated by Delft3D-QUICKIN Module according to the actual seabed topography. In the sensitivity experiments, we will apply several different water depths to test the corresponding response of the tidal wave and flow.

Open boundary conditions are prescribed by a large-scale China Sea model. 8 main tidal constituents are specified along the open boundary of the schematized model as the drive forcing for the water motion.

2.2. *Model performance*

The simulation period of the model is set to one month with a time step of 3 minutes considering for a stable and accurate computation (Courant number < 10). Tidal dynamic pattern is shown by co-tidal chart and tidal ellipse field of M_2 constituent in the whole domain (Figure 2). The amphidromic point (AP) which has a significant influence on the local tidal pattern is simulated by this schematized model. Also, along the central Jiangsu coastline and RSRF area, the amplitude is increased greatly, forming a zone of large amplitude about 1.8m. This feature is similar to the actual tidal characteristics of RSRF area (Chen et al., 1992). The tidal ellipse field displays that the tidal currents show a great potential moving convergent and divergent towards one center (focal point of the radial current, referred to FP in the following of this paper), which is the city of Jianggang in reality. In the north of Jiangsu coast (area A in Figure 2), the tidal current is mostly the reciprocating flows. However, outside the Yangtze River Estuary and south of radial sand ridges (area B and C in Figure 2, respectively), the tidal current ellipse type is rotary.

In order to assess the schematized model, we compared the results with previous literatures and

observations (Table 1). Here we only listed the position of the AP and FP of the current field off the central Jiangsu Coast. Table 1 shows that the amphidromic system as well as the tidal current field simulated by the schematized model differ little from both the results of previous tidal wave models with real geometries and the observation. The difference is mainly due to the deviation between different calculation methods. So, our model has a good agreement with the previous results in the RSRF and South Yellow Sea, and has the capacity to conduct numerical experiments. Besides, the good agreements also show that the resolution of the coastline has less effect on the tidal dynamics, because even under the condition of the regular coastline shape, the tidal dynamics is still hardly changed.

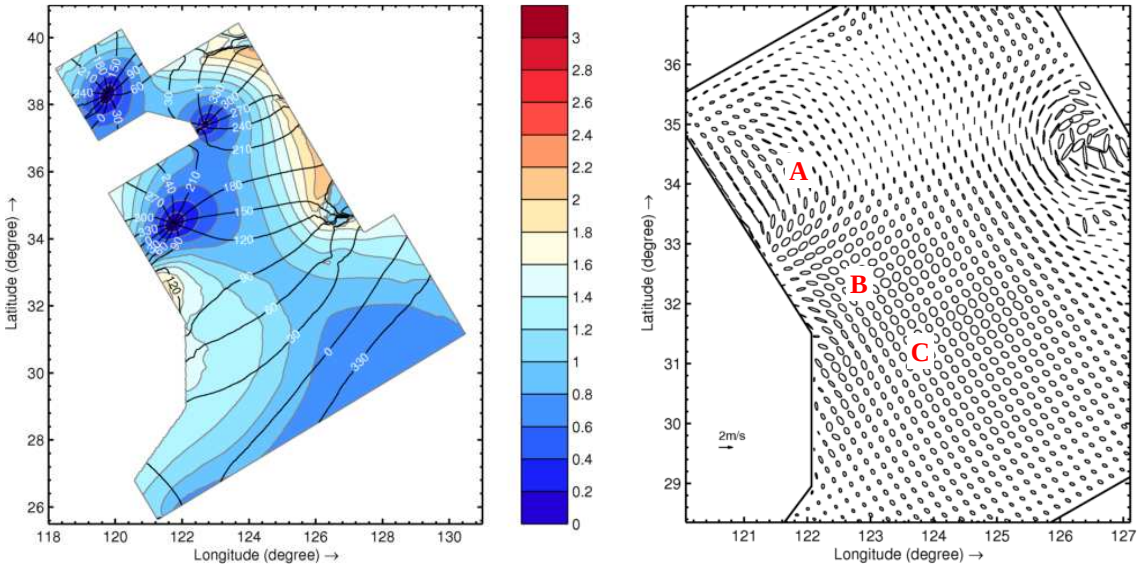

Figure 2. Co-tidal chart of M_2 constituent (Left) and tidal ellipse field of M_2 constituent focusing on the South Yellow Sea (Right)

Table 1. Comparison between the results and the previous studies.

Models	Position of AP	Position of the FP
Schematized model (this paper)	121°45′E, 34°27′N	121°30′E, 32°30′N
Marine Atlas (Chen et al., 1992) (Observation)	121°33′E, 34°15′N	121°12′E, 32°29′N
Fang (1986) (Chinese sea model)	121°40′E, 34°40′N	--
Zhang (2005) (Chinese Sea model)	121°26′E, 34°34′N	121°06′E, 32°50′N
Xing (2011) (South Yellow Sea model)	121°38′E, 34°38′N	121°00′E, 32°41′N

3. Sensitivity Experiment Results And Discussion

In order to get a more clear knowledge about tidal current along the Jiangsu coast, a series of experiments based on this schematized model are designed and conducted. Two factors which are hypothesized to be responsible for the radial tidal current pattern are investigated: the shape of the coastline, and the submarine topography. The aim of these experiments is to analyze the dominant factor which is responsible for the formation and evolution of this radial tidal current. In this section, the effects of these factors are described in detail.

3.1. *The shape of coastline*

The shape of coastline includes two parts: from a view of small scale, it indicates the irregular geological settings along the real coastline, such as estuaries, bay, etc. Under such context, these settings do influence the local tidal current patterns on either direction or magnitude of the flow velocity during tidal cycles, because the shape of the closed boundary imposes restrictions on the water motions and further influence

the local flow. While from the results of the schematized model simulation, it seems the response of tidal dynamics in large scale to these irregular coastlines is less obvious. On the other hand, from a large scale view, the Chinese marginal seas can be simplified as a large tidal basin with only one open boundary in the south (Figure 1). On this condition, the influence of large-scale change of the basin boundaries may influence the tidal wave pattern, but the effect of this kind of coastline shape on the tidal dynamics is still uncertain. Thus, in this section, we mainly focus on the influence of the shape of the tidal basin boundaries to the tidal dynamics based on the schematized model.

We carried out numerical experiments on the response of the tidal dynamics of different geometric configurations. Three different land boundaries of a tidal basin are designed (Figure 3). Case 1 changes the Chinese coastline to a straight line; case 2 is closing the Bohai Sea and case 3 is omitting North Yellow Sea to finally make the basin to a rectangular basin.

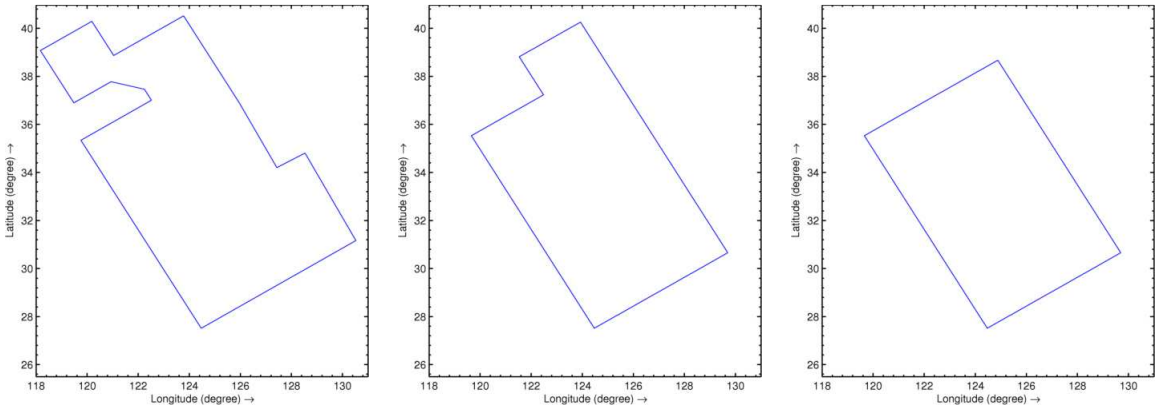

Figure 3. Different geometric configurations of the domain (from left to right: case 1, case 2 and case 3).

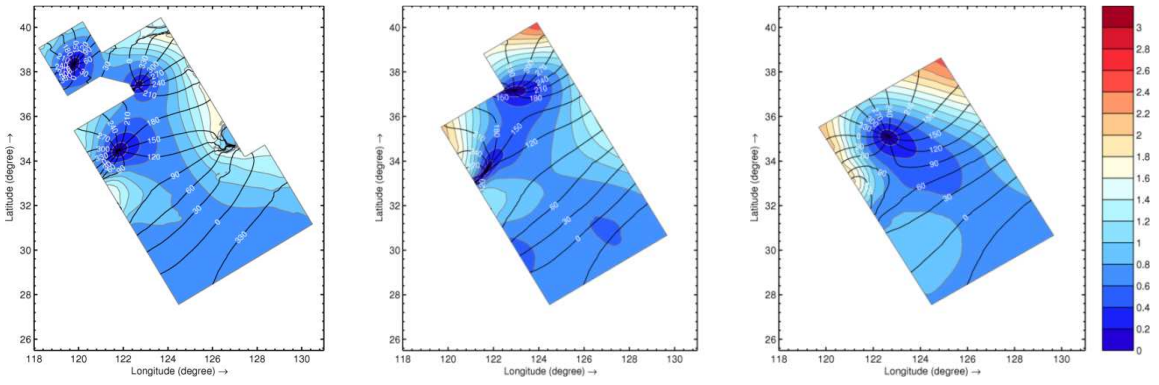

Figure 4. Co-tidal charts of M_2 constituent in the three cases (from left to right: case 1, case 2 and case 3). Note: black lines are co-phase lines and the background coloured patches are the co-amplitude map.

The co-tidal charts of the M_2 constituent for these 3 cases are shown in Figure 4, and the corresponding tidal wave pattern can be displayed through these figures. Compared with the original schematized model (Figure 2), the tidal wave propagation pattern of case 1 changes very little and basically the same as the original one. For example, there are three amphidromic points with little difference of theirs positions. The amplitude in the RSRF area is a little less than the original model, because the incoming tidal energy reduced due to the decrease of the open boundary in case 1. Compared with case 1, the co-phase lines of 0°, 30°, 60°, 90° in case 2 near the open boundary is unchanged, that is to say, the incident tidal wave pattern is not influenced after closing the Bohai Sea. But the co-phase lines changed a lot in the northern area. The amphidromic points in North Yellow Sea and South Yellow Sea are both shifting southward and the one in the South Yellow Sea become more flat compared with case 1. That is because Bohai Sea is closed in case 2, there is no energy dissipating to the Bohai Sea and the tidal wave energy become larger in both North Yellow Sea and South Yellow Sea. This will strengthen the reflected tidal wave resulting in the shifting of

the amphidromic points southward. Furthermore, the flat shape of the amphidromic system in the South Yellow indicates that the superposition between the enhanced reflected tidal wave and the incident tidal wave become more complete. And the amplitude in RSRF area turned to be smaller. In case 3, closing the North Yellow Sea make the domain to be a complete rectangular basin, and the tidal wave has a typical feature of a tidal system in the semi-enclosed rectangular basin. The position of the amphidromic point in the South Yellow Sea shifted eastward close to the center axis of the domain, which show a large area of rotating tidal wave system. The co-phase lines near the open boundary gradually parallel to the north land boundary which is different with the previous cases, maybe because the reflected tidal wave becomes bigger and further influences the incident tidal wave. In this case, the co-amplitude lines near the China Coast become basically parallel to the coastline with largest magnitude in the north corner. This feature is in accordance with the analytical solutions of the semi-enclosed rectangular basin. It should be noted that this large amplitude area is different with the former two cases, in which the shape of the area is an enclosed half-circle (Figure 4).

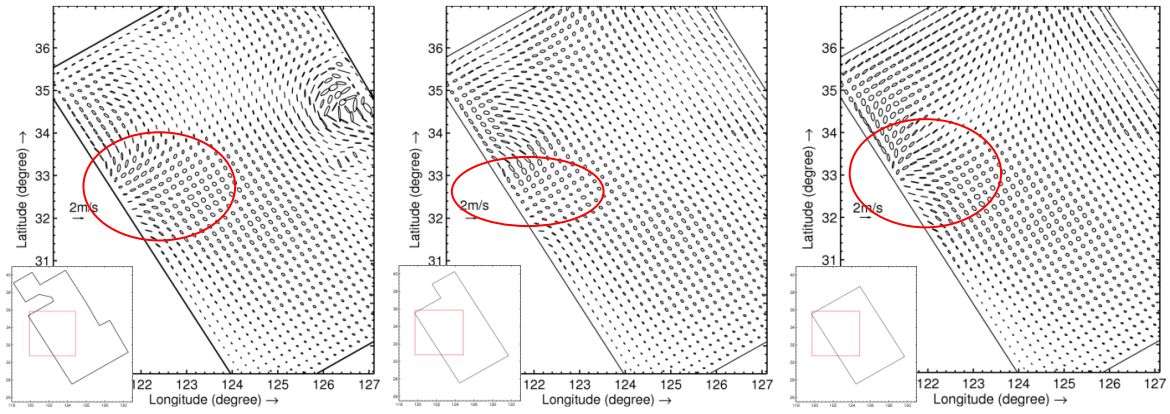

Figure 5. Tidal ellipse field of M_2 constituent in the three cases (from left to right: case 1, case 2 and case 3).

Figure 5 is the tidal ellipse fields which represent the tidal current patterns of these 3 cases. In case 1, the radiating pattern of the tidal current in the RSRF area is kept, whereas in case 2, both the range and the magnitude of the radial current field reduced in consistency with the flat amphidromic system. In case 3, the radial tidal current pattern appears again and the magnitude of the tidal ellipse is bigger than in case 1. The response of the tidal current pattern to the different geometric configurations is inconsistent with the tidal wave, because in Figure 4, the 90° co-phase line in the central Jiangsu coast is enclosed which implies the water convergent in that area. In fact, according to the rectangular tidal wave theory, the enclosed co-phase lines will exist in the distance of ¼ wavelength of the incident tidal wave to the north boundary. So, even there are no Bohai Sea and the North Yellow Sea, the radial tidal current field still exist. Compared with the tidal wave pattern, the tidal current is less sensitive to the change of geometric configuration of the tidal basin.

The averaged tidal energy flux per unit width is calculated in order to find the deep reasons which cause the changes of both tidal wave and current pattern (Figure 6). In case 1, the tidal energy flux is relatively large on the side of Korean Peninsula, while on the side of the China coast, the tidal energy is small due to the Shandong Peninsula which cause the tidal wave reflected and dissipated. This pattern is consistent with the reality. But when we closed the Bohai Sea, the tidal wave energy in the North Yellow Sea decreased clearly. This shows that the dissipation effect is strengthened in the North Yellow Sea if no energy penetrates into Bohai Sea. The tidal energy which is expected to enter the Bohai Sea then enhance the reflect tidal wave. This reinforced tidal wave meeting the incident tidal wave is the main reason causing the decrease of the total tidal wave energy in the North Yellow Sea. Additionally, the tidal energy fluxes in the southern Shandong Peninsula (area A in Figure 6) and northern Jiangsu Coast (area B in Figure 6) are increased in case 2 compared with case 1. This indicates that the shifting of the amphidromic system in North Yellow Sea can enhance the tidal energy in the area off Jiangsu Coast, which enhance the local reflected wave caused by Shandong Peninsula. This can explain the tidal amphidromic system become flat leading to small area of radial current field in RSRF area in case 2. Furthermore, compared with the co-

tidal chart and tidal energy flux figure of the case 2, the results also imply that the amphydromic system in the South Yellow Sea is not only depending on the local tidal wave propagating schema and local geometry, but also has more or less relationship with amphidromic system in the North Yellow Sea. So, the shape of the geometric boundary could influence the radial current pattern in RSRF through affecting the tidal wave propagating scheme. In case 3, the tidal energy flux is mainly following the east and north boundary, and an anti-clockwise circulation of the energy flux in the Northern domain is clearly shown in Figure 6. This anti-clockwise circulation is consistent with the amphidromic tidal wave system.

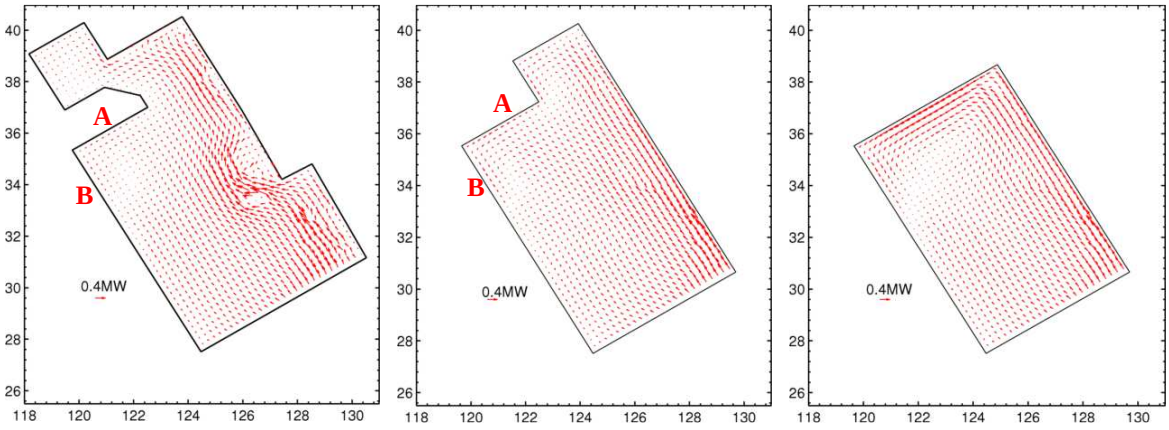

Figure 6 Tidal energy flux per unit width (from left to right: case 1, case 2 and case 3).

In summary, the amphidromic system in the South Yellow Sea is sensitive to the north land boundaries, while the radial current field is less sensitive. Additionally, the amphidromic system in the South Yellow Sea is not only caused by the reflected tidal wave from the Shandong Peninsula, but also controlled by the tidal wave system in the North Yellow Sea.

3.2. *Submarine bathymetry in the surrounding seas*

In the previous studies, the influence of the topography to the tidal current field is limited to the local area. It is suggested that the tidal current field is independent of the radial sand ridges because in the condition of flat bottom instead of radial sand ridges, the radial tidal current field still exists. We think the surrounding seas bathymetry may have influence on the local tidal current pattern although the local bathymetry has less effect.

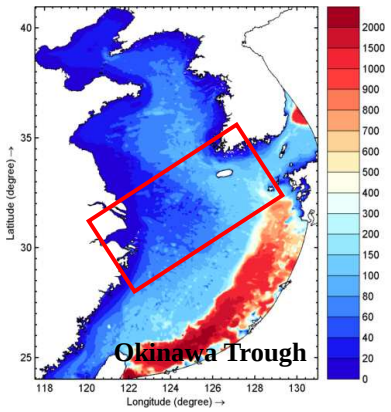

Figure 7. Bathymetry of the Chinese marginal sea

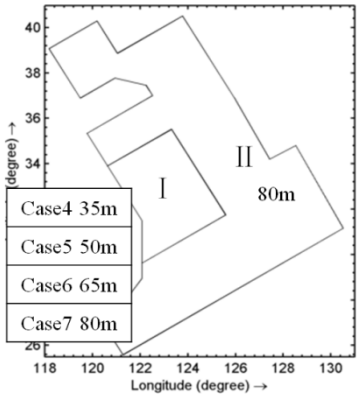

Figure 8. Sensitive cases on the influence of the lateral water depth

Figure 7 is the bathymetry map of the Chinese marginal seas. Through this map, we find that the topography of the Chinese marginal seas shows a step-like characteristic: the water depth become smaller

from south to north and from center to both sides. In the junction area of the East China Sea and South Yellow Sea, there is a lateral depth difference shown in the red box of Figure 7. The water depth near the Chinese coast is about 40m, while it is 90 m in the area close to Korean Peninsula. This difference in the lateral direction may influence the tidal wave propagation into the basin. Besides, the trend of the Okinawa Trough has an angle with the basin. This angle will make the tidal wave travel much faster along the Korean Peninsula than along the Chinese coast. So, the effects of the lateral water depth difference and the trend of the deep trough are investigated here.

3.2.1 *Lateral difference of the water depth*

First we designed several experiments to explore the lateral depth influence. The model domain was divided into 2 parts (Figure 8). And in part 1, four different water depths are applied and in part 2, the depth is set to uniform, 80m. So, from case 4 to case 7, the lateral differences of the water difference is 45m, 30m, 15m, and 0m respectively. Through this method, we can find under which difference the special tidal current pattern will exist.

Figure 9 shows the co-tidal charts of M_2 constituent. The amphidromic systems in these four cases are basically the same, while shifted to the center of the basin compared to the original model. This is due to the applied uniform depth in the most area of the domain and the friction effects are decreased. The co-phase lines near open boundary suggest that the incoming tidal wave propagate fastest when there are no lateral water depth in case 7, while smaller in case 4 when the difference is 45m. And in the middle of the domain, the co-phase lines of the four cases are basically the same, which indicate that the tidal wave pattern is relatively same in all cases. For the amplitude in RSRF region, only case 4 and case 5 show there have large amplitude area, around 1.6m, which implies that the flow have the tendency to convergent to this place. That is to say, under the lateral difference of the water depth of either 45m or 30m, the tidal wave pattern might be similar to the reality.

Figure 10 displays the tidal ellipse field in the four cases. It can be seen that in case 4, in the area where the water depth in part one is 35m, the tidal current ellipticities are large and have a tendency towards China coast, which is in a good agreement with the real tidal current field. But in the near shore zone, the magnitude of the tidal current is relatively small. That is because the water depth in local area should be very shallow in reality, while in the model simulation it is set to a uniform value 35m. And in case 5, the tidal ellipse field is not very obvious tending towards to the RSRF zone nor in the cases 6 and 7. The pattern of the tidal current corresponding to the tidal wave pattern is analyzed according to the co-tidal map. So, the lateral depth difference is at least about 45m, the radial current could be generated in RSRF area. In fact, the depth in the Chinese marginal seas can satisfy this condition, which means the depth difference indeed influence the tidal current pattern.

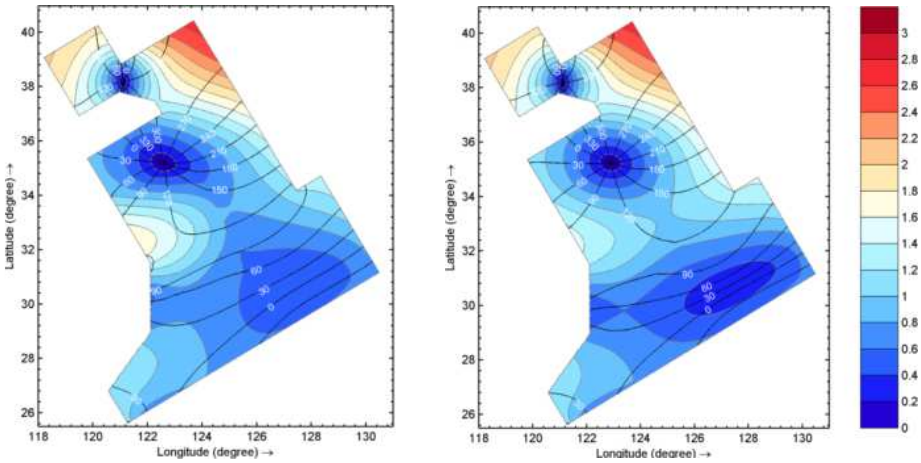

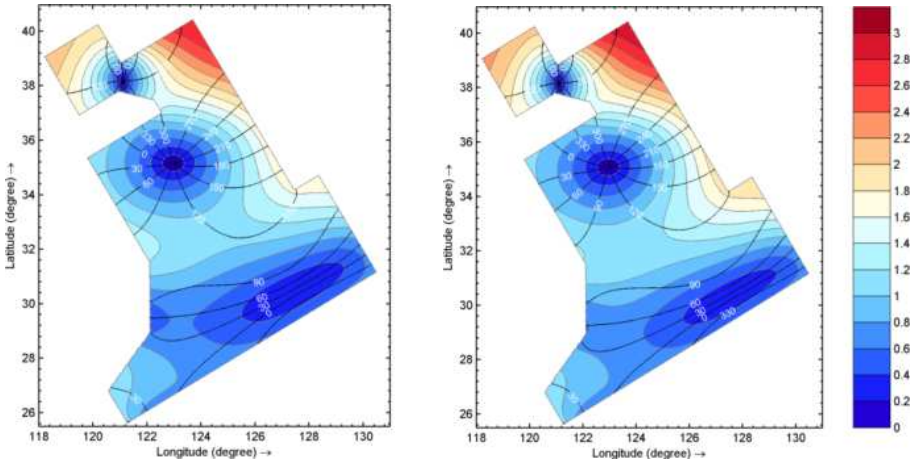

Figure 9. Co-tidal charts of M_2 constituent (from left to right, and top to bottom: case 4,case 5, case 6 and case 7).

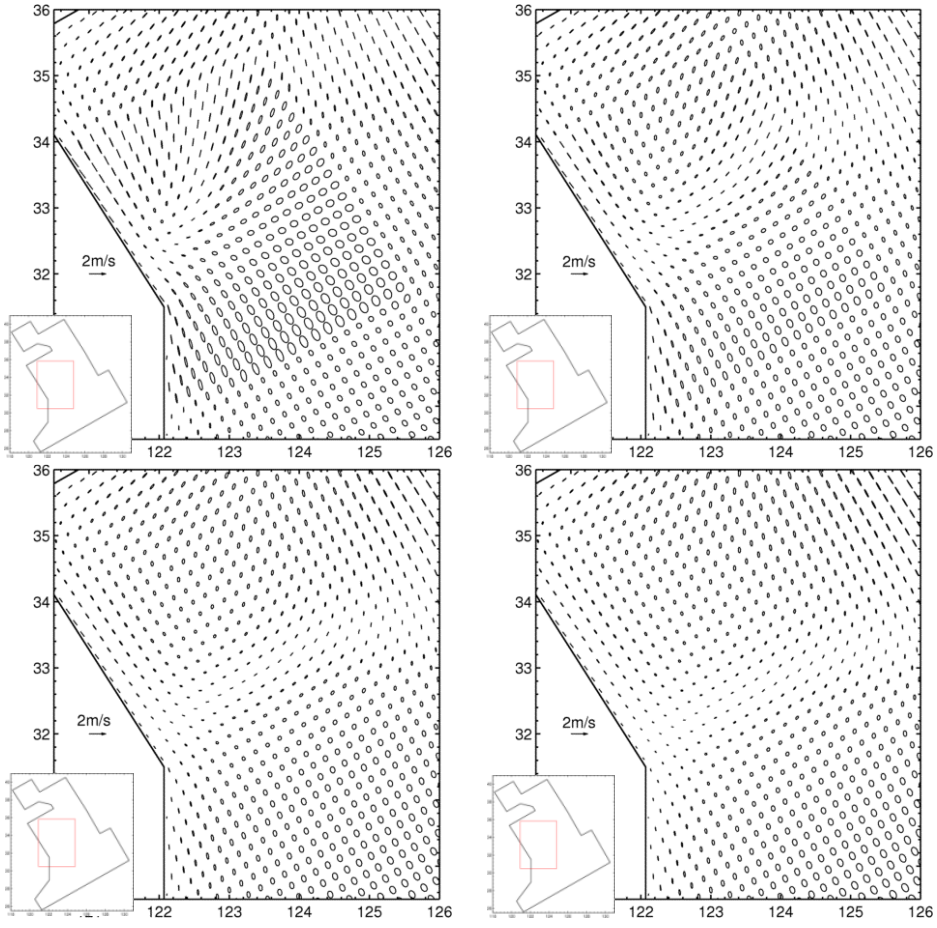

Figure 10. Tidal ellipse field of M_2 constituent in case 4 to case 7, from left to right and top to bottom, respectively.

3.2.1 *Okinawa Trough*

In order to explore the effect of the deep trough near the open boundary, we carried out another experiment. In case 8, the uniform water depth is applied in the East China Sea leaving the other zones unchanged (Figure 11). This method can neglect the influence of the deep Okinawa but considering the lateral depth difference in the conjunction area of the East China Sea and the Yellow Sea.

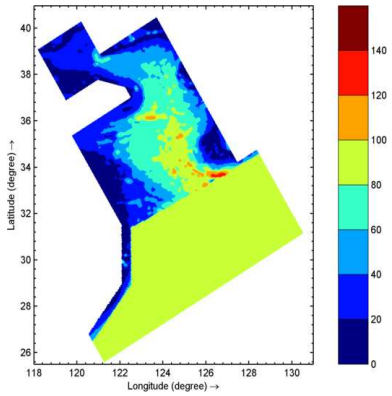

Figure 11. Bathymetry of the domain in case 8

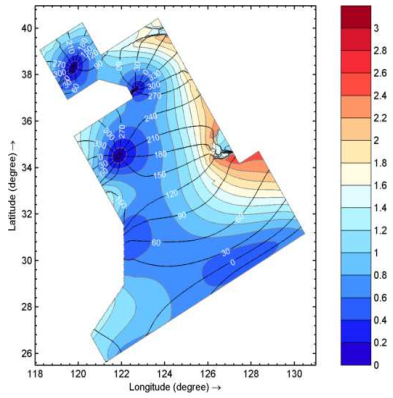

Figure 12. Co-tidal chart of M_2 constituent of case 8

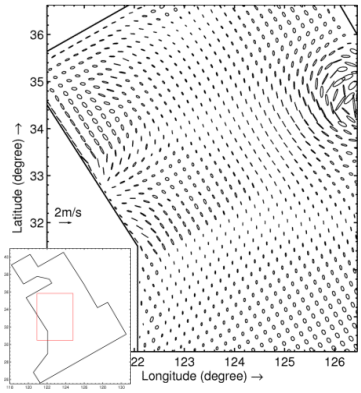

Figure 13. Tidal ellipse field of M_2 constituent of case 8

The results are shown as the form of the co-tidal charts and tidal current ellipse field in Figure12 and Figure 13, respectively. From Figure 12, it can be seen that in the southern domain, the co-phase lines are parallel to the open boundary when there are no deep trough. The tidal wave propagates as the same pattern in both sides. And in the area of RSRF, the amplitude is relatively large as well. Another important finding is that in the area of Yangtze Estuary, a degenerated amphidromic point can be distinguished. And it is also noted that the distance between the amphidromic point in the South Yellow Sea and this degenerated one should be corresponded to half of wavelength of M_2 tidal wave, which depend on the water depth of the South Yellow Sea. In figure 13, the radial tidal current field can be found, but with a relatively small magnitude and range. So, this phenomenon confirms our hypothesis about the lateral depth difference, even under the condition of the same tidal wave in both sides. On the other hand, the magnitude and range of the field may be influenced by the presence of the Okinawa Trough.

At last, we combine the effect of these two factors and conduct a new case. In case 9, we apply a new bathymetry to the model simulation, which is to simplify the topography of the whole domain to a step-like one based on the two influence factors (Figure 14). Uniform water depth is applied in each colored patches.

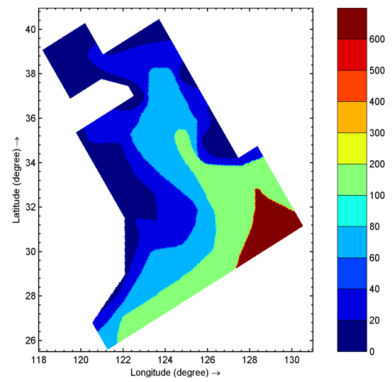

Figure 14. Step-like bathymetry in case 9

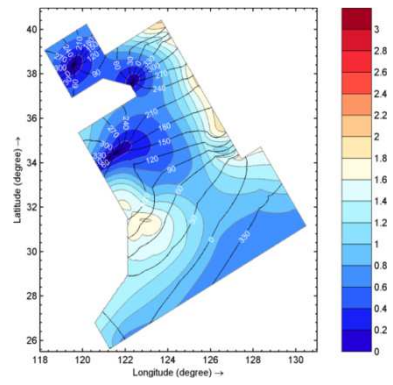

Figure 15. Co-tidal chart of M_2 constituent in case 9

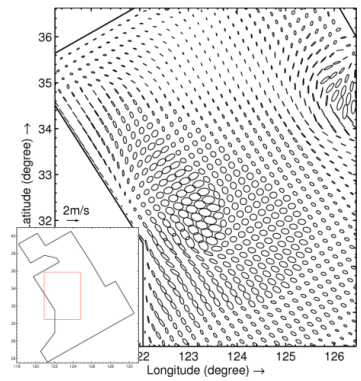

Figure 16. Tidal ellipse field of M_2 constituent of case 9

The new bathymetry includes the two factors, while neglecting the small scale variations on the sea bed. Figure 15 is the co-tidal chart calculated with the new bathymetry. It can be seen that the tidal wave pattern in case 9 has a reasonable agreement with the original model. The position of the amphidromic point is 121°30′E, 34°24′N, is slightly different than in the original model which gives the position 121°45′E, 34°27′N. And the co-phase lines and the area of the large amplitude in RSRF are both consistent with the reality. The tidal wave pattern calculated with this idealized bathymetry is still representing the basic characteristics of the actual tidal wave pattern. Meanwhile, the tidal ellipse field (Figure 16) also shows a large area of radiating features in the central Jiangsu Coast with a relatively large magnitude. So, in

summary, the surrounding seas water depth is indeed important on the existence of the radial current field. The lateral depth difference affect the existence of the radial current field and the distribution of the trough influence the range and the magnitude of the current field.

4. Conclusion

In this paper, a schematized numerical model is developed to investigate the influence factors and the formation mechanism of the radial tidal current field in the central Jiangsu Coast. The schematized model combining the method of numerical simulations and influence factors analysis with reference to analytical solutions can provide sufficient information about the tidal dynamic mechanism on the whole Chinese marginal sea. The effect of different shapes of the shoreline and surrounding sea topography are then examined in detail in numerical experiments.

Firstly, the geological settings along the land boundary, or irregular coastlines of China, have less influence on both tidal wave pattern and tidal current field. For the geometric configuration of the basin, we considered three different basin shape and the corresponding effects. For example, the shape of southern China coastline is not the elongation of the Jiangsu coastline but turning toward west (Figure 1). This breakpoint on the Yangtze Estuary may cause tidal current flow around the area (diffraction of tidal wave) and this may influence the formation of the radial tidal current. But according to results of case 1, these features of the coastline have no relation with the radial current pattern in RSRF area. Further the results suggest that the shape of the north boundary have a significant influence on the tidal wave pattern, while relatively small impact on the tidal current field. Besides, we find that the amphydromic system in the South Yellow Sea is not only generated because of the refection effect of Shandong Peninsula, but also influenced by the tidal wave system in the North Yellow Sea.

For the influence of the topography, it has been demonstrate that the lateral water depth and the trend of the Okinawa Trough indeed has considerable influence on the tidal dynamics according to the results of the numerical experiments. The trend of the Okinawa Trough cause the tidal wave propagates faster on the side of Korean Peninsula than that along the China Coast. The lateral difference of the tidal wave propagation will be further amplified by the lateral water depth difference. This lateral difference of the tidal wave propagation can increase the lateral effect of the Poincare waves, shown in Figure 16 as the large ellipticities area. According to this mechanism, the tidal current in southern (affected by the Poincare waves) and northern (controlled by the amphidromic system) RSRF area will come together in RSRF area and converge to one radiating flow and finally caused formation of the radial current pattern.

Finally, the roles of the geometric shoreline shape and water depth of the basin mainly manifested in two aspects: influence the wavelength and limit the propagating pattern of the incoming tidal wave. And then further influence on the tidal current pattern in the RSRF area. That is to say, if the incoming tidal wave is defined, the position of the AP as well as the FP is fixed in a basin with specified geometric shape and submarine topography. In fact, according to Yu (1995), the shelves of Yellow Sea and East China Sea were exposed as a part of land during the period of late Quaternary. After that period, the global temperature rise and the glaciers start melting which caused the sea-level rise again. Then, the ocean started to pour into this area and gradually submerged the lower continental shelves. In other words, the topography of Yellow Sea and East China Sea has been exposed out of water for a relatively long period. After the sea-level rise, the interaction between tide and the Shelf bathymetry caused the change of sediment transportation and formed the present topography. So, the pattern of the radial current in RSRF area is the inevitable result of the tidal wave propagation over this particular topography and geometric shape of the shoreline.

Acknowledgements

The first author is financially supported by the China Scholarship Council. This study was additionally supported by the 111 Project of the Ministry of Education and the State Administration of Foreign Experts Affairs, China (Grant No. B12032).

References

Chen D., Sun X., Pu Y., 1992.*Marine Atlas of Bohai Sea, Yellow Sea and East China Sea (Hydrology).* China Ocean Press (in Chinese).

Fang G., 1979. Dissipation.of tidal energy in Yellow Sea. *Oceanologia Et Limnologia Sinica,* 10: 200-213 (in Chinese).

Fang G., 1986. Tide and tidal current charts for the marginal seas adjacent to China. *Chinese Journal of Oceanology and Limnology,* 4, 1-16.

Jung, K.T., Park, C.W., Oh, I.S., So, J.K., 2005. An analytical model with three sub-regions for M_2 tide in the Yellow sea and the East China Sea. *Ocean Science Journal*, 40: 191-200.

Kang, Y.Q., 1984. An analytic model of tidal waves in the Yellow Sea. *Journal of Marine Research* 42: 473-485.

Lesser, G.R., Roelvink, J.A., Van Kester, J.A.T.M., Stelling, G.S., 2004. Development and validation of a three-dimensional morphological model. *Coastal Engineering*, 51: 883-915.

Li, C., Li, B., 1981. Studies on the Formation of Subei Sand Cays. *Oceanologia Et Limnologia Sinica*, 12: 321-331 (in Chinese).

Liu, Z., Xia, D., 2004. *Tidal Sands in China Seas*, Ocean Press (in Chinese).

Ren, M., Xu, Y., Zhu, J., 1986. *Comprehensive Investigation of the Coastal Zone and Tidal Land Resources of Jiangsu Province,* Ocean Press, Beijing (in Chinese).

Song, Z., Yan, Y., Xue, H., Mao, L., 1998. Hydromechanics for formation and development of radial sandbanks-II vertical characteristics of tidal flow. *Science in China (Series D)*, 28: 411-417 (in Chinese).

Taylor, G.I., 1922. Tidal oscillations in gulfs and rectangular basins. *Proceedings of the London Mathematical society,* 2: 148-181.

Wan, Y., Zhang, Q., 1985. The source and movement of sediments of radiating sand ridges off Jiangsu Coast. *Oceanologia Et Limnologia Sinica,* 16: 392-399 (in Chinese).

Wang, Y., 2003. *Radiative Sandy Ridge Field on Continental Shelf of the Yellow Sea.* China Environmental Science Press, Beijing (in Chinese).

Xing, F., Wang, Y.P., Wang, H.V., 2011. Tidal hydrodynamics and fine-grained sediment transport on the radial sand ridge system in the southern Yellow Sea. *Marine Geology*.

Yang, C., 1985. On the origin of Jianggang radial sand ridges in Yellow Sea. *Marine Geology & Quaternary Geology*, 5: 35-44 (in Chinese).

Ye A., Chen Z., 1987. Effect of bottom topography on tidal amphydromic system in semi-enclosed rectangular waters. *Journal of Shandong College of Oceanology,* 17:1-7 (in Chinese).

Yu H., Liu J., 1995. Advances in study of China's Shelf quaternary geology. *Advances in Earth Sciences*, 10(6): 531-536 (in Chinese).

Zhang, C., Zhang, D., Zhang, J., Wang, Z., 1999. Tidal current-induced formation—storm-induced change—tidal current-induced recovery. *Science in China Series D: Earth Sciences*, 42: 1-12.

Zhang, D., Zhang, J., 1996. M2 Tidal wave in the Yellow Sea radiate shoal region. *Journal of Hohai University (Natural Sciences)*, 24: 35-40 (in Chinese).

Zhang, G., 1991. Formation and evolution of sand ridges in the South Huanghai Sea Shelf. *Marine Geology & Quaternary Geology*, 11: 25-35 (in Chinese).

Zhang, J., Li, C., 1999. Producing condition and evolving progress of the tidal sand bodies in the Northern Jiangsu and the Southern Huanghai Sea. *Acta Oceanologica Sinica*, 21: 65-74 (in Chinese).

Zhang W., 2005. *Numerical Modeling of Tides Wave in Margin Seas Near China*. Hohai University (in Chinese).

Zhu, Y., 1998. Numerical simulation of Paleo-tidal current field in the Subei littoral plain area and its verification. *Marine Science Bulletin*, 17: 1-7 (in Chinese).

Zhu, Y., Chang, R., 1997. Explanation of the origin of radial sand ridges in the Southern Yellow Sea with numerical simulation results of tidal currents. *Journal of Ocean University of Qingdao*, 27: 218–224 (in Chinese).

Zhu, Y., Chang, R., 2001. Sediment dynamics study on the origin of the radial sand ridges in the Southern Yellow Sea. *Studia Marina Sinica*, 43: 38-50 (in Chinese).

Zhu, Y., Li, C., Chang, R., 1995. Numerical explanations on genesis of the Jianggang radial sandbanks with relevance of ancient eviroment. *Journal of Tongji University,* 23: 226-230 (in Chinese).

Zhu, Y., Yan, Y., 1998. Tidal Current Numerical Model for the Formation and Development of Radial Sandbank in the Yellow Sea. *Journal of Hydrodynamics: A Series*, 13: 473-480 (in Chinese).

Zhu, Y., Yan, Y., Xue, H., 1998. Hydromechanics for Formation and Development of Radial Sandbanks I Plane Characteristics of Tidal Flow. *Science in China (Series D),* 28: 403‑410 (in Chinese).